

2012

# Intrinsic Magnetic Properties of L10-Based Mn-Al and Fe-Co-Pt Alloys

P. Manchanda

*University of Nebraska - Lincoln*

Ralph Skomski

*University of Nebraska at Lincoln, rskomski2@unl.edu*

Jeffrey Shield

*University of Nebraska at Lincoln, jshield@unl.edu*

S. Constantinides

*Arnold Magnetic Technologies*

Arti Kashyap

*The LMN Institute of Information Technology, akashyap@lnmiit.ac.in*

Follow this and additional works at: <http://digitalcommons.unl.edu/physicsskomski>

---

Manchanda, P.; Skomski, Ralph; Shield, Jeffrey; Constantinides, S.; and Kashyap, Arti, "Intrinsic Magnetic Properties of L10-Based Mn-Al and Fe-Co-Pt Alloys" (2012). *Ralph Skomski Publications*. Paper 88.

<http://digitalcommons.unl.edu/physicsskomski/88>

This Article is brought to you for free and open access by the Research Papers in Physics and Astronomy at DigitalCommons@University of Nebraska - Lincoln. It has been accepted for inclusion in Ralph Skomski Publications by an authorized administrator of DigitalCommons@University of Nebraska - Lincoln.



## Intrinsic Magnetic Properties of $L1_0$ -Based Mn-Al and Fe-Co-Pt Alloys

P. MANCHANDA,<sup>1)</sup> R. SKOMSKI,<sup>2)</sup> J. E. SHIELD,<sup>3)</sup> S. CONSTANTINIDES,<sup>4)</sup> and A. KASHYAP<sup>1)</sup>

<sup>1)</sup> *Department of Physics, The LNM Institute of Information Technology, Jaipur, Rajasthan, India 302031, and School of Basic Sciences, Indian Institute of Technology Mandi, Himachal Pradesh, India 175001.*

<sup>2)</sup> *Department of Physics and Astronomy and NCMN, University of Nebraska, Lincoln, NE 68588.*

<sup>3)</sup> *Department of Mechanical and Materials Engineering, University of Nebraska, Lincoln, NE 68588.*

<sup>4)</sup> *Arnold Engineering, 770 Linden Avenue, Rochester, NY.*

**Abstract** — Density functional theory is used to investigate how atomic substitutions modify the magnetization and anisotropy of  $L1_0$ -ordered ferromagnets. Our VASP supercell calculations focus on two classes of materials: Mn-Al-(Fe) and Fe-Co-Pt. We find that the Mn and Al moments in pure MnAl are  $2.420 \mu_B$  and  $-0.61 \mu_B$  per atom, respectively. The calculated zero temperature anisotropy is  $1.77 \text{ MJ/m}^3$ . Replacing 50% of Mn by Fe enhances the anisotropy from  $1.77 \text{ MJ/m}^3$  to  $2.50 \text{ MJ/m}^3$  but reduces the magnetization. We have also calculated the magnetic moments of  $L1_0$ -ordered  $\text{Fe}_{1-x}\text{Co}_x\text{Pt}$  with various degrees of Fe-Co disorder. Configurational supercell averaging shows that the net moment decreases systematically with Co concentration, but the individual Fe and Co moments depend on the number of Fe-Co bonds.

### I. INTRODUCTION

The ongoing search for rare-earth free permanent magnets has led to a renewed interest in  $L1_0$ -ordered alloys. Their use as permanent magnets has been limited so far not only by the price of heavy transition metals (Pd, Pt) but also by the modest 3d magnetization in MnAl and MnBi [1, 2]. This paper deals with the origin and magnitude of the local magnetic moments in  $L1_0$ -type magnetic compounds.

Figure 1 shows a unit cell of the most general  $L1_0$  structure, which has the nominal composition  $\text{ABC}_2$ . Very often, the A atoms (black) and B atoms (gray) are of the same type, which yields an equiatomic composition, but different A and B atoms are also compatible with the tetragonal symmetry of the  $L1_0$  structure [3].

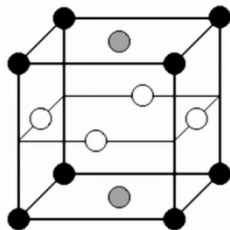


Fig. 1. General  $L1_0$  structure of the composition  $\text{ABC}_2$ .

$L1_0$ -ordered MnAl, also known as  $\tau$ -phase MnAl, is one of the few ferromagnetic manganese alloys [4, 5] and exhibits appreciable intrinsic properties, namely  $\mu_0 M_s = 0.75 \text{ T}$ ,  $K_1 = 1.7 \text{ MJ/m}^3$ , and  $T_c = 650 \text{ K}$  [1, 2]. These are

somewhat inferior to the intrinsic properties of FePt and CoPt, but both Mn and Al are cheap and readily available. Aside from permanent magnets,  $\tau$ -phase MnAl is of interest for magnetic tunnel junctions (MTJs) [6].

A disadvantage of  $\tau$ -phase MnAl is the structural instability at room temperature [7]. This leads to elaborate processing techniques, such as quenching from the hexagonal high-temperature ( $\epsilon$ ) phase, which is antiferromagnetic with  $T_N$  of 90 K [8]. However, small additions of carbon are well-known to drastically improve the stability of the  $L1_0$  phase [9].

An important thrust of  $L1_0$  research is iron-series transition-metal substitutions aimed at improving magnetization, anisotropy, and/or Curie temperature. In non-cubic Fe-rich Pt alloys, a reduction of raw-materials costs can be achieved by substituting iron-series transition metals for expensive heavy 4d/5d transition-metal elements. For example, magnetizations of up to 1.78 T and coercivities of up to 2.52 T have been achieved in Fe-Co-Pt thin films with moderately reduced Pt content [10, 11]. In MnAl alloys, it has been found that Fe addition enhances the Curie temperature [12].

From a theoretical point of view, the coherent potential approximation (CPA) has been used to investigate various substitutions in  $L1_0$  compounds containing Pt and Pd [13, 14]. Our emphasis is on local atomic magnetic moments, which we determine with VASP supercell calculations. The atomic moments are important for the understanding of the magnetism of magnetic alloys but difficult to



determine experimentally. Furthermore, the CPA is a single-site approach and therefore ignores cluster-effects [3, 15]. This means that nonrandom atomic neighborhoods ("clusters") are not accounted for very well. In this paper, we consider atomic magnetic moments in  $L1_0$  structures and focus on two systems, namely Mn-Al-Fe and  $\text{Fe}_{1-x}\text{Co}_x\text{Pt}$ .

## II. COMPUTATIONAL DETAILS

We have used the frozen core full potential projected augmented wave (PAW) method [16], as implemented in the Vienna *ab-initio* simulation package (VASP) [17]. The electronic exchange and correlation effect are described within the generalized-gradient approximation (GGA), using the functional proposed by Perdew *et al.* [18]. The energy cutoff of the plane wave basis set is taken as 450 eV and the total energy of the system is converged to  $10^{-4}$  eV for all the structures. To determine the magnetization for MnAl alloys, the experimental lattice constants are used ( $a = 3.93 \text{ \AA}$ ,  $c = 3.56 \text{ \AA}$ ) [4].

For Fe-Mn-Al alloys we replace 50% of the Mn in MnAl by Fe, corresponding to the structure shown in Fig. 1. The Fe-Co-Pt supercells, which contain of 32 atoms (8  $L1_0$  unit cells per supercell), will be explained in Sect. III, and in the calculations we assume experimental lattice constants for FePt ( $a = 3.861 \text{ \AA}$  and  $c = 3.788 \text{ \AA}$ ) [19]. The  $k$ -points meshes for Brillouin zone sampling were constructed using the Monkhorst-pack scheme. To ensure a reasonable accuracy, all calculations use a  $11 \times 11 \times 11$  mesh generating 126  $k$ -points in the irreducible part of Brillouin zone. For some of the systems we have also performed magnetic-anisotropy calculations and then used 2197  $k$ -points in the irreducible part of Brillouin zone to ensure convergence.

## III. Fe-SUBSTITUTED MnAl

For the  $L1_0$  MnAl alloys, we obtain Mn and Al moments of  $2.420 \mu_B$  and  $-0.061 \mu_B$ , respectively. This means that the coupling between the Mn and Al sublattices is antiferromagnetic. Replacing 50% of the Mn by Fe reduces the total magnetization of the system. In this case, the magnetic moments of Fe, Mn and Al are  $2.461 \mu_B$ ,  $1.899 \mu_B$ , and  $-0.056 \mu_B$ , respectively. Figure 2, shows the spin-resolved density of states (DOS) for the Fe-Mn-Al system. As usual, the magnetic moment corresponds to the difference in the  $\uparrow$  and  $\downarrow$  DOS.

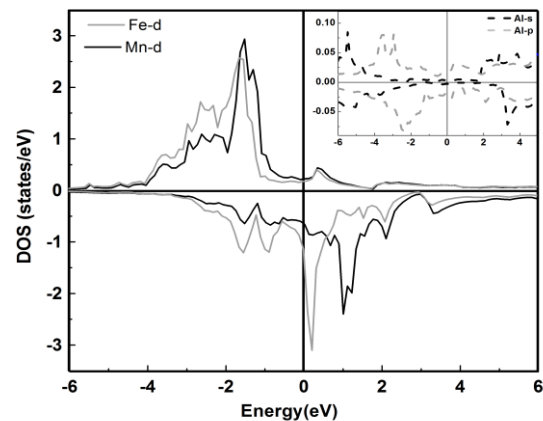


Fig. 2. Spin-polarized majority ( $\uparrow$ ) and minority ( $\downarrow$ )  $d$  densities of states (DOS) of  $\text{FeMnAl}_2$ . The inset shows the  $s$  and  $p$  DOS of Al.

We have also calculated the zero-temperature magnetic anisotropy of MnAl alloys is  $K_1 = 1.77 \text{ MJ/m}^3$ , which is consistent with previous experimental and theoretical results [20, 21]. The Fe substitution enhances the anisotropy constant from  $1.77 \text{ MJ/m}^3$  to  $2.5 \text{ MJ/m}^3$  [ $25 \text{ Mergs/cm}^3$ ].

## III. Fe-Co-Pt ALLOYS

In the second part of the calculations, we have investigated several ordered and disordered ternary  $L1_0$ -based Fe-Co-Pt alloys. We have considered 4 types of ordered alloys, all having the nominal composition  $\text{Fe}_8\text{Co}_8\text{Pt}_{16}$  but differing by their stackings, both vertically and laterally. The two configurations shown in Fig. 3 are limiting cases with respect to the dominance of Fe-Fe, Co-Co, and mixed Fe-Co nearest-neighbor bonds. Figure 3(a) is basically the same as Fig. 1, whereas Fig. 3(b) is a multilayer. The intermediate configurations, not discussed in this paper, require the full supercell to achieve periodicity and yield intermediate moments.

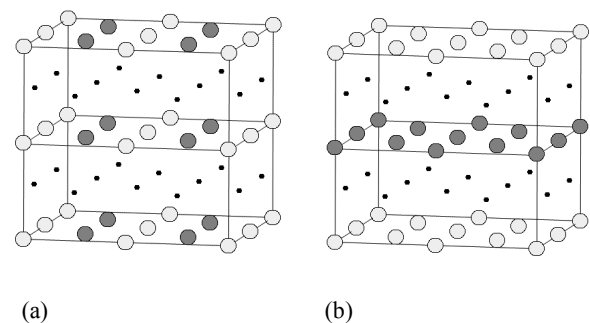


Fig. 3. Two of the ordered  $L1_0$ -based Fe-Co-Pt alloys considered in the calculations: (a)  $L1_0$  limit and (b) (multi)layered limit.

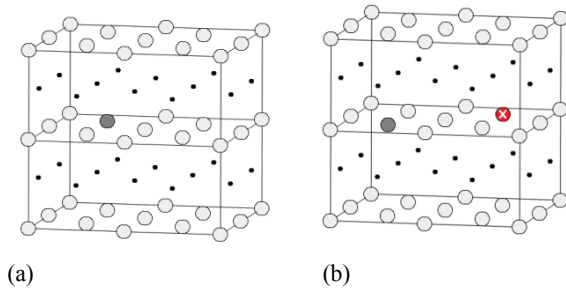


Fig. 4. Supercell configurations for disordered  $\text{Fe}_{1-x}\text{Co}_x\text{Pt}$ : (a)  $x = 6.25\%$  and (b)  $x = 12.5\%$ . There are 7 nonequivalent configuration for  $x = 12.5\%$ , but only one of them is shown in (b).

The structure of *disordered* Fe-Co-Pt alloys requires a more detailed explanation. These alloys are also approximated by supercells with 32 atoms, Fig. 4, and have the nominal compositions  $\text{Fe}_{15}\text{CoPt}_{16}$  ( $x = 6.25\%$ ) and  $\text{Fe}_{14}\text{Co}_2\text{Pt}_{16}$  ( $x = 12.5\%$ ). In  $\text{Fe}_{15}\text{CoPt}_{16}$ , Fig. 4(a), there are 16 possible Co sites, because the Co is assumed to replace one of the Fe atoms, but all Co sites are crystallographically equivalent. In the  $\text{Fe}_{14}\text{Co}_2\text{Pt}_{16}$  supercell, there are 15 possibilities to accommodate the second Co atom, but only 7 of these configurations are crystallographically non-equivalent. Figure 3(b) shows one of them.

Each nonequivalent configuration requires a separate first-principle calculation, and the net moment  $\langle m_X \rangle$  ( $X = \text{Fe}, \text{Co}, \text{Pt}$ , total) is then determined by configurational averaging. For  $\text{Fe}_{14}\text{Co}_2\text{Pt}$ , this means that

$$\langle m_X \rangle = \frac{1}{15} \sum_{i=1}^7 w(i) m_X(i) \quad (1)$$

Here  $i = 1 \dots 7$  labels the non-equivalent configurations and the  $w(i)$  are their weights, normalized to  $\sum w(i) = 15$ .

Table I summarizes the calculated atomic moments. For comparison, we also calculated the magnetic moment of binary  $L1_0$  FePt and CoPt, and the results are consistent with previously calculated magnetic moments [22]. The effective Fe-Co moment in  $\text{Fe}_8\text{Co}_8\text{Pt}_{16}$  alloys is  $2.42 \mu_B$ . Similar values were reported for  $\text{Fe}_{0.55}\text{Co}_{0.45}/\text{Pt}$  superlattice ( $2.5 \mu_B$ ) [23] and three-dimensional  $\text{Fe}_{0.56}\text{Co}_{0.44}$  nanoparticles [24].

Note that the  $L1_0$ -ordered and layered structures (Fig. 3) have nearly exactly the same total moments. However, the relative Fe and Co contributions are different. In particular, the Fe moments are larger in the  $L1_0$  structure (a) than in the layered structure (b). This is consistent with the general trend of reduced magnetization (moment and exchange) in dense-packed Fe structures [2].

Table I. Magnetic moments of  $L1_0$  Fe-Co-Pt ordered and disordered alloys. The standard deviation (SD) in the last row refers to the configurational averaging over the 7 nonequivalent sites.

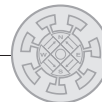
	Supercell	$\langle m_{\text{Co}} \rangle$	$\langle m_{\text{Fe}} \rangle$	$\langle m_{\text{Pt}} \rangle$
	Fig.	$\mu_B$	$\mu_B$	$\mu_B$
$L1_0$ -ordered $\text{Fe}_8\text{Co}_8\text{Pt}_{16}$	3(a)	1.805	3.034	0.390
Layered $\text{Fe}_8\text{Co}_8\text{Pt}_{16}$	3(b)	1.921	2.915	0.393
Disordered $\text{Fe}_{15}\text{Co}_1\text{Pt}_{16}$	4(a)	1.852	2.907	0.367
Disordered $\text{Fe}_{14}\text{Co}_2\text{Pt}_{16}$	4(b)	1.857	2.919	0.372
$\text{Fe}_{14}\text{Co}_2\text{Pt}_{16}$ SD	4(b)	0.012	0.0017	0.0007

An alternative view is to consider that Fe is fairly close to the middle of the 3d series, intermediate between Cr and Mn (typically antiferromagnetic) and Co and Ni (typically ferromagnetic). This introduces a pronounced real-structure dependence into the magnetism of the Fe. Cobalt is much more stable in this regard, but it nevertheless strongly hybridizes with neighboring atoms. In fact, the Co moments in the different  $\text{Fe}_{14}\text{Co}_2\text{Pt}_{16}$  configurations vary from  $1.831$  to  $1.879 \mu_B$ , and the standard deviation of the Co moments ( $0.012 \mu_B$ ) is larger than those for Fe and Pt. The Pt moment reflects the spin polarization due to neighboring Fe and Co moments—Pt is a well-known exchange-enhanced Pauli paramagnet that gets easily spin-polarized. The induced moment per Pt atom ranges from about  $0.3 \mu_B$  to  $0.4 \mu_B$ .

#### IV. DISCUSSION

The reduction of the MnAl magnetization due to Fe substitution is not surprising, because Mn exhibits a strong tendency towards antiferromagnetism in most atomic environments. Structural changes in ferromagnetic Mn alloys, such as MnAl and the hexagonal compound MnBi [9, 25], cause the antiferromagnetism to resurface. This may even lead to more complicated types of magnetic order, such as noncollinear spin structures, which have not been investigated here.

One advantage of the present supercell method is the automatic consideration of cluster localization [15]. In the supercell approach, such neighborhood effects are properly taken into account, and supercell calculations can safely be



used for all degrees of randomness. The downside is that the number atomic configurations increase exponentially with system size and number of impurity atoms.

Nevertheless, the present calculations are in good agreement with available CPA calculations, indicating that cluster localization is not very important from a practical point of view. We have found, however, that the local magnetic moments exhibit a subtle dependence on the environment, not only in each Fe-Co layer but also through alternating 4d/5d layers. The effect is rather small, of the order of 0.01  $\mu_B$  per atom, but substantially contributes to the standard deviation shown in Table I.

Both supercell and CPA calculations indicate that the average moment *decreases* with increasing Co content. This is different from bcc Fe<sub>1-x</sub>Co<sub>x</sub>, where the moment initially increases with *x*, from 2.2  $\mu_B$  (Fe) to 2.4  $\mu_B$  (Fe<sub>65</sub>Co<sub>35</sub>). The difference between Fe-Co and Fe-Co-Pt is a band-structure effect—bcc Fe-Co and dense-(fcc-like) Fe-Co-Pt behave very differently in this regard.

## V. CONCLUSIONS

In summary, we have used a supercell method to determine magnetic properties of *L*<sub>10</sub>-ordered MnAl(Fe) and Fe<sub>1-x</sub>Co<sub>x</sub>Pt. The Mn and Al moments in pure MnAl are 2.420  $\mu_B$  and -0.061  $\mu_B$  per atom, respectively, which means that the coupling between Mn and Al sublattices is antiferromagnetic. The calculated zero-temperature magnetic anisotropy is 1.77 MJ/m<sup>3</sup>. Replacing 50% of Mn by Fe enhances the anisotropy from 1.77 MJ/m<sup>3</sup> to 2.5 MJ/m<sup>3</sup>, but reduces the magnetization.

Supercell calculations capture details not accounted for in the CPA but require a configurational averaging and get very time-as the supercell size increases. In the Fe-Co-Pt system, the magnetic moments of Co and Fe show a relatively strong dependence on the number of Fe-Co nearest neighbors. In disordered Fe<sub>14</sub>Co<sub>2</sub>Pt<sub>16</sub> alloys, the respective Fe and Co moments increase and decrease with increasing Fe-Co disorder, whereas 3*d*-3*d* interactions through the Pt layer yield minor corrections.

## ACKNOWLEDGMENT

This research is supported by ARPA-E REACT (PM, RS, SC), BREM (JES), and DST (AK). The authors are grateful to P. K. Sahota, L. H. Lewis, and D. J. Sellmyer for stimulating discussions.

## REFERENCES

- [1] T. Klemmer, D. Hoydick, H. Okumura, B. Zhang, and W. A. Soffa, *Scripta Met. Mater.* **33**, 1793 (1995).
- [2] R. Skomski and J. M. D. Coey, *Permanent Magnetism*, Institute of Physics, Bristol 1999.
- [3] R. Skomski, *J. Appl. Phys.* **101**, 09N517 (2007).
- [4] H. Kono, *J. Phys. Soc. Japan* **13**, 1444 (1958).
- [5] A. J. J. Koch, P. Hokkelling, M.G.V.D. Sterg, K. J. DeVos, *J. Appl. Phys.* **31**, 75S (1960).
- [6] M. Hosoda, M. Oogane, M. Kubota, T. Kubota, H. Saruyama, S. Iihama, H. Naganuma, and Y. Ando, *J. Appl. Phys.* **111**, 07A324 (2012).
- [7] Y. Kurtulus, R. Dronskowski, *J. Solid State Chem.* **176**, 390 (2003).
- [8] K. Kamino, T. Kawaguchi, and M. Nagakura, *IEEE Trans. Magn.* **2**, 506 (1966).
- [9] J. E. Evetts, ed., *Concise Encyclopedia of Magnetic and Superconducting Materials*, Pergamon, Oxford, 1992.
- [10] P. K. Sahota, Y. Liu, R. Skomski, P. Manchanda, R. Zhang, M. Franchin, H. Fangohr, G. C. Hadjipanayis, A. Kashyap, and D. J. Sellmyer, *J. Appl. Phys.* **111**, 07E345 (2012).
- [11] Y. Liu, T. A. George, Ralph Skomski, and D. J. Sellmyer, *Appl. Phys. Lett.* **99**, 172504 (2011).
- [12] C. Paduani, J. Schaf, A. I. C. Persiano, J. D. Ardisson, *J. Alloys Compounds* **479**, 1 (2005).
- [13] M. E. McHenry, B. Ramalingum, S. Willoughby, J. MacLaren, and S. G. Sankar, *IEEE Trans. Magn.* **37**, 1277 (2001).
- [14] S. Willoughby, J. MacLaren, T. Ohkubo, S. Jeong, M. E. McHenry, D. E. Laughlin, S.-J. Choi and S.-J. Kwon, *J. Appl. Phys.* **91**, 8822 (2002).
- [15] E. N. Economou, *Green's Functions in Quantum Physics*, Springer, Berlin 1979.
- [16] G. Kresse, and D. Joubert, *Phys. Rev. B* **59**, 1758 (1999).
- [17] G. Kresse and J. Hafner, *Phys. Rev. B* **48**, 13115 (1993).
- [18] Y. Wang and J. P. Perdew, *Phys. Rev. B* **44**, 13298 (1991).
- [19] P. Villars and L. D. Calvert, *Pearson's Handbook of Crystallographic Data for Intermetallic Phase* (Meta Park, OH, ASM, 2000).
- [20] A. Sakuma, *J. Phys. Soc. Japan* **63**, 1422 (1994).
- [21] J. H. Park, Y. K. Hong, S. Bae, J. J. Lee, J. Jalli, G. S. Abo, N. Neveu, S. G. Kim, C. J. Choi, and J. G. Lee, *J. Appl. Phys.* **107**, 09A731 (2010).
- [22] A. Kashyap, R. Skomski, A. K. Solanki, Y. F. Xu, and D. J. Sellmyer, *J. Appl. Phys.* **95**, 7480 (2004).
- [23] G. Andersson, T. Burkert, P. Warnicke, M. Björck, B. Sanyal, C. Chacon, C. Zlotea, L. Nordström, P. Nordblad, and O. Eriksson, *Phys. Rev. Lett.* **96**, 037205 (2006).
- [24] A. Kleibert, J. Passig, K.-H. Meiwes-Broer, M. Getzlaff, and J. Bansmann, *J. Appl. Phys.* **101**, 114318 (2007).
- [25] J. B. Goodenough, *Magnetism and the Chemical Bond*, Wiley, New York 1963.